Progress In Electromagnetics Research, PIER 80, 277–293, 2008

STUDY ON SCINTILLATION CONSIDERING INNER- AND OUTER-SCALES FOR LASER BEAM PROPAGATION ON THE SLANT PATH THROUGH THE ATMOSPHERIC TURBULENCE

Z.-S. Wu, H.-Y. Wei, R.-K. Yang, and L.-X. Guo

School of Science
Xidian University
Xi'an 710071, China

Abstract—Based on both the modified Rytov method and the altitude-dependent model of the ITU-R slant atmospheric turbulence structure constant, the uniform model of scintillation index considering inner- and outer-scales is derived form weak to strong fluctuation regions with Gaussian beam propagation on the slant path, and can be degenerated to the result of the horizontal path with atmospheric structure constant is a fixed value. The numerical conclusions indicate the smaller wavelength, the inner-scale has a stronger impact on scintillation than outer-scale. But, in strong fluctuation, the outer-scale effect is prominence. Finally, the numerical results are compared and verified with the experimental data.

1. INTRODUCTION

As an optical beam propagates through the atmosphere, it will experience random deflections due to scintillation and beam spreading and so on. Basic scintillation characteristics have been studied for 60 years. In the late 1950s, Tatarskii and Chernov adopted Rytov approximation method [1–4] and introduced the modern statistic theory of turbulence. They obtained the Rytov results of plan wave and sphere wave in the weak turbulence, which are still the classic theory on wave propagation in weak fluctuation region. The limitation of the weak fluctuation theory was clearly demonstrated and saturation phenomenon of the scintillation was discovered by the experimental data of Gracheva and Gurvich [5, 6] in 1965, neither the Born approximation nor Rytov approximation can explain the experiments. So many scholars explored theoretically and hoped to explain the characteristics of wave propagation in strong turbulence.

The modified Rytov method expanded the above study to the moderate and strong turbulences [7–9]. According to Rytov covariance $\sigma_0^2 = 1.23 C_n^2 k^{7/6} L^{11/6} \gg 1$ of plan wave in the strong turbulence, Fante obtained the intensity fluctuation variance σ_I^2 of plan wave with asymptotic theory [10, 11], but this result was lower than Gracheva and Gurvich's experimental data obviously. Reference [12] offered the approximate expression of intensity fluctuation variance in the saturation area, with and without considering the influence of inner-scale. To sphere wave, without the consideration, the result were lower than the experimental data in the reference [13]. However, with the consideration, the result was much closer to it. So, on the study of optical scintillation, the influence of inner-scale should be taken in turbulence area, esp. the saturation area of strong fluctuation. In 1993, Miller [14] developed the analysis of scintillation index of Gaussian beam in weak fluctuation area. In 1999, Cynthia et al. [15] studied and intensity fluctuation variance of Gaussian beam propagation on horizontal path in the saturation area. Andrews et al. [7] have developed the scintillation index models with finite inner- and outer-scale for a plane, spherical and beam wave, which can be applied to moderate-to-strong regions. There are many correlative researches [16–20] and application [21] of turbulent model. A.Kuramoto et al. [22] given laser speckle imaging of a finger by scattered light optic. Many excellent reviews related to optical wave propagation [23] in the ionosphere [24, 25] and other medium [26–30] have been published.

Based on the altitude-dependent model of the ITU-R turbulence structure constant model, the modified Rytov method, which applicable to the optical wave propagation on the horizontal path, is extended to the propagation on the slant path. This paper derives the uniform model of scintillation index considering inner- and outer-scales form weak to strong fluctuation regions with Gaussian beam propagation through atmospheric turbulence on the slant path, and can be degenerated to the result of the horizontal path with atmospheric structure constant is a fixed value. The effect of different inner- and outer-scales to Gaussian beam scintillation propagation on slant path is discussed. Finally, the numerical results are compared and verified with the experimental data.

2. SCINTILLATION INDEX CONSIDERING INNER- AND OUTER-SCALES

2.1. Modified Rytov Theories on Slant Path

Atmospheric turbulence structure constant which is altitude dependent is general statistic nonhomogeneous. Based on modified Rytov method, we introduce the ITU-R turbulence structure constant model [31] on the slant path expressed as

$$\begin{aligned} C_n^2(h) = &\ 8.148 \times 10^{-56} v_{RMS}^2 h^{10} e^{-h/1000} \\ &+2.7 \times 10^{-16} e^{-h/1500} + C_0 e^{-h/100} \end{aligned} \tag{1}$$

There $v_{RMS} = \sqrt{v_g^2 + 30.69 v_g + 348.91}$ is the wind velocity of vertical path, v_g is sub aerial wind velocity, C_0 is sub aerial atmospheric structure constant (its typical value is $1.7 \times 10^{-14}\mathrm{m}^{-2/3}$).

We start with the following modified Rytov method assumptions: (1) Atmospheric turbulence is statistic nonhomogeneous. (2) The received irradiance of an optical wave can be modeled as a modulation process in which small-scale (diffractions effect) are multiplicatively modulated by large-scale (refractive effect) fluctuations. (3) Small- and large-scale processes are statistically independent, as $I = xy$ (x, y are the effect genes of large- and small-scale of turbulence to intensity, respectively). (4) The Rytov method for optical scintillation is valid even into the saturation regime with the introduction of a spatial coherence of the optical wave in strong fluctuation regimes. (5) The geometrical optics method can be applied to large-scale irradiance fluctuations. Under the approximate of modified Rytov method, the optical wave propagation between the source and receiver is given by

$$U(r,\, L) = U_0(r,\, L) \exp\left[\psi_x(r,\, L) + \psi_y(r,\, L)\right] \tag{2}$$

where $\psi_x(r,\, L)$ and $\psi_y(r,\, L)$ are independent and statistic uncorrelated complex phases random, and correspond to the effect of the large- and small-scale of turbulence. L is the propagation path length between transmitter and receiver, r is observe position in the observe plane, $U_0(r,\, L)$ is the optical field distribution with turbulence nonexistence.

In fact, the intensity fluctuation of optical wave propagation in space is dependently on space refractive index fluctuation spectrum. Introducing the inner- and outer-scales of turbulence to the Kolmogorov spectrum model can expand its effective range. Although this rebuild model is experience, the results obtained by this modified model are closer to experimental data than Kolmogorov spectrum model. Considering the inner- and outer-scales effect of atmospheric turbulence, and based on the Kolmogorov spectrum model, Andrews et al. introduce a spatial frequency filter function. Hence, the effective spectrum of refractive-index fluctuations [9, 15] can be expressed as

$$\Phi_{nG}(\kappa,\, l_0,\, L_0) = \Phi_n(\kappa) G(\kappa,\, l_0,\, L_0) \tag{3}$$

where $\Phi_n(\kappa) = 0.033 C_n^2 \kappa^{-11/3}$ is Kolmogorov spectrum, k is the optical wave number.

The spatial filter function is

$$\begin{aligned} G(\kappa,\, l_0,\, L_0) &= G_x(\kappa,\, l_0,\, L_0) + G_y(\kappa) \\ &= f(\kappa,\, l_0) g(\kappa,\, L_0) \exp\left(-\frac{\kappa^2}{\kappa_x^2}\right) + \frac{\kappa^{11/3}}{\left(\kappa^2+\kappa_y^2\right)^{11/6}} \end{aligned} \tag{4}$$

$$\begin{aligned} f(\kappa,\, l_0) = &\exp\left(-\kappa^2/\kappa_l^2\right)\left[1+1.802(\kappa/\kappa_l) - 0.254(\kappa/\kappa_l)^{7/6}\right] \\ &\kappa_l = 3.3/l_0 \end{aligned} \tag{5}$$

In Eq. (4), the parameter κ_x is a lager-scale (or refractive) spatial frequency cutoff much like an inner-scale parameter and κ_y is a small-scale (or diffractive) spatial frequency cutoff much like an outer-scale parameter. In this fashion, $G_y(\kappa)$ is the high-pass filter function (spatial frequency $\kappa > \kappa_y$) and $G_x(\kappa,\, l_0,\, L_0)$ is the low-pass filter function (spatial frequency $\kappa < \kappa_x$), at a given propagation distance. Where $g(\kappa, L_0)$ is the outer-scale factor, as following

$$g(\kappa,\, L_0) = 1 - \exp\left(-\frac{\kappa^2}{\kappa_0^2}\right) \quad (\kappa_0 = 8\pi/L_0) \tag{6}$$

Substituting Eq. (6) into Eq. (4), the low-pass filter function can be written as

$$\begin{aligned} G_x(\kappa,\, l_0,\, L_0) &= G_x(\kappa,\, l_0) + G_x(\kappa,\, L_0) \\ &= f(\kappa,\, l_0) \exp\left(-\frac{\kappa^2}{\kappa_x^2}\right) - f(\kappa,\, l_0) \exp\left(-\frac{\kappa^2}{\kappa_x^2}\right) \exp\left(-\frac{\kappa^2}{\kappa_0^2}\right) \end{aligned} \tag{7}$$

Based on beam characteristics, the scintillation variance of a Gaussian beam wave is composed of beam radial and longitudinal (or axis) component and takes the form

$$\sigma_I^2(r,\, L) = \sigma_{I,r}^2(r,\, L) + \sigma_{I,l}^2(0,\, L) \tag{8}$$

This is obtained by supposing the small-scale fluctuations are multiplicatively modulated by large-scale fluctuations. The radial component of scintillation vanishes on the laser beam axis ($r = 0$) and is closely approximated by the radial log-variance [2, 9]

$$\sigma_{I,r}^2(r, L) \cong \sigma_{\ln I,r}^2(r, L) \cong 4.42\sigma_0^2\Lambda_e^{5/6}\frac{r^2}{W_e^2} \quad r \leq W \tag{9}$$

where W is the free-space radius of beam at the receiver, Λ_e and W_e is effective receiver beam parameter.

$$\begin{aligned} \Lambda_e &= \frac{\Lambda}{1+1.625\sigma_1^{12/5}\Lambda} = \frac{\Lambda}{1+4q\Lambda/3} = \frac{2L}{kW_e^2}, \\ W_e &= W\left(1+1.625\sigma_0^{12/5}\Lambda\right)^{1/2} \end{aligned} \tag{10}$$

In strong fluctuations, the radial component will diminish eventually as the beam propagations into the saturate region except, possibly, at $r \gg W$. This paper mainly studies long-distance laser propagation on the slant path, so its radial component does not make an excessive discussion here.

Under general atmospheric conditions, the radial component of a Gaussian beam wave scintillation index is [32]

$$\sigma_{I,l}^2(L) = \exp\left(\sigma_{\ln I,l}^2\right) - 1 \cong \sigma_{\ln I,l}^2 \quad \sigma_0^2 \ll 1 \tag{11}$$

where $\sigma_{\ln I,l}^2$ is the log-irradiance variance. Considering the inner- and outer-scale, Eq. (11) can be expressed as

$$\begin{aligned} \sigma_{\ln I,l}^2 = \ & 8\pi^2k^2L\int_0^1\int_0^\infty \kappa\Phi_{nG}\left(\kappa,\, l_0,\, L_0\right)\exp\left(-\Lambda L\kappa^2\xi^2/k\right) \\ & \left\{1-\cos\left[\frac{L\kappa^2}{k}\xi(1-\bar{\Theta}\xi)\right]\right\}\mathrm{d}\kappa\mathrm{d}\xi \end{aligned} \tag{12}$$

Here, z is propagation distance, $\xi = z/L$, Λ and $\bar{\Theta}$ are receiver beam parameters defined by

$$\begin{aligned} \Lambda = \frac{\Lambda_0}{\Lambda_0^2+\Theta_0^2} &= \frac{2L}{kW^2},\ W = W_0(\Theta_0^2+\Lambda_0^2)^{1/2},\ \Theta_0 = 1-\frac{L}{R_0} \\ \bar{\Theta} &= 1-\frac{\Theta_0}{\Theta_0^2+\Lambda_0^2}, \quad \Lambda_0 = \frac{2L}{kW_0^2} \end{aligned} \tag{13}$$

where W_0 is the beam radius and R_0 is the phase front radius of curvature at the transmitter.

Substituting Kolmogorov spectrum into Eq. (12), the Rytov variance on slant path [15] for Gaussian beam is shown as

$$\sigma_{1,B}^2 = 1.83\sigma_0^2 \int_0^1 \frac{C_n^2(\xi H)}{C_{n0}^2} \xi^{\frac{5}{6}} (1 - \bar{\Theta}\xi)^{\frac{5}{6}} \mathrm{d}\xi \tag{14}$$

where $k = 2\pi/\lambda$, λ is the wavelength of the incidence wave.

Based on the third assumption, and considering the effect of the large- and small-scale turbulent eddies to scintillation index, which is defined as

$$\begin{aligned}\sigma_{I,l}^2(l, L) &= < x^2 >< y^2 > -1 = (1 + \sigma_x^2)(1 + \sigma_y^2) - 1 \\ &= \sigma_x^2 + \sigma_y^2 + \sigma_x^2\sigma_y^2\end{aligned} \tag{15}$$

Moreover, the σ_x^2 and σ_y^2 in the Eq. (15) can be expressed in terms of log-irradiance variances of x and y as $\sigma_x^2 = \exp(\sigma_{\ln x}^2) - 1$, $\sigma_y^2 = \exp(\sigma_{\ln y}^2) - 1$. The Eq. (15) is written as

$$\sigma_{I,l}^2(l, L) = \exp\left(\sigma_{\ln x}^2 + \sigma_{\ln y}^2\right) - 1 \tag{16}$$

These theories are applicable under weak-to-strong irradiance fluctuations. So, the longitudinal (axis) component of scintillation index of the Gaussian beam considering inner- and outer-scale is

$$\sigma_{I,l}^2(l, L) = \exp\left(\sigma_{\ln x, l_0}^2 - \sigma_{\ln x, L_0}^2 + \sigma_{\ln y}^2\right) - 1 \tag{17}$$

where $\sigma_{\ln x, l_0}^2$ is large-scale log irradiance fluctuation variance considering inner-scale, $\sigma_{\ln x, L_0}^2$ is large-scale log irradiance fluctuation variance considering outer-scale, $\sigma_{\ln y}^2$ is small-scale log irradiance fluctuation variance.

2.2. Small-scale Log Irradiance Fluctuation Variance

Based on modified Rytov and Gaussian beam optical scintillation theory, the small-scale log irradiance fluctuation is as follows [3]

$$\begin{aligned}\sigma_{\ln y}^2 = \ & 8\pi^2 k^2 L \int_0^1 \int_0^\infty \kappa \Phi_n(\kappa) G_y(\kappa) \exp\left(-\Lambda_e L \kappa^2 \xi^2 / k\right) \\ & \left\{1 - \cos\left[\frac{L\kappa^2}{k} \xi \left(1 - \bar{\Theta}\xi\right)\right]\right\} \mathrm{d}\kappa \mathrm{d}\xi\end{aligned} \tag{18}$$

Submitting the expression of atmospheric refracting index spectrum $\Phi_n(\kappa)$ and small-scale filter function $G_y(\kappa)$ into Eq. (18).

Applying $1 - \cos\alpha \approx 1$, and there is

$$\sigma^2_{\ln y} \approx 2.605k^2 L \int_0^1 C_n^2(\xi H) \int_0^\infty \frac{\kappa}{(\kappa^2+\kappa_y^2)^{11/6}} \exp\left(-\Lambda L\kappa^2\xi^2/k\right) \mathrm{d}\kappa \mathrm{d}\xi \tag{19}$$

Let $\eta = L\kappa^2/k$, $\eta_y = L\kappa_y^2/k$, then Eq. (19) can be written as

$$\sigma^2_{\ln y} = 1.303k^2 L C_{n0}^2 \int_0^1 \frac{C_n^2(\xi H)}{C_{n0}^2} \int_0^\infty \left(\frac{L}{k}\right)^{5/6} [\eta+\eta_y]^{-11/6} \exp(-\Lambda\eta\xi^2)\mathrm{d}\eta\mathrm{d}\xi \tag{20}$$

When $\Lambda\eta\xi^2 \ll 1$ and $\exp(-\Lambda\eta\xi^2) \approx 1$, Eq. (20) is given by

$$\sigma^2_{\ln y} \approx 1.06\sigma_0^2 \int_0^1 \frac{C_n^2(\xi H)}{C_{n0}^2} \int_0^\infty [\eta+\eta_y]^{-11/6} \mathrm{d}\eta\mathrm{d}\xi \tag{21}$$

Simplified Eq. (21), the small-scale log-irradiance variance is shown as

$$\sigma^2_{\ln y} \approx 1.27\sigma_G^2 \eta_y^{-5/6} \tag{22}$$

where considering inner scale effect, η_y is the cutoff frequency of filter function without dimension, namely

$$\eta_y = 3 + 2.07\sigma_G^{12/5} \tag{23}$$

σ_G^2 is log-irradiance fluctuation variance under weak fluctuation on slant path, can be expressed as

$$\sigma_G^2 = 8\pi^2 k^2 L \int_0^1 \int_0^\infty \kappa\Phi_n(\kappa) f(\kappa,\, l_0) \exp\left(-\Lambda L\kappa^2\xi^2/k\right) \left\{1 - \cos\left[\frac{L\kappa^2}{k}\xi\left(1-\bar{\Theta}\xi\right)\right]\right\} \mathrm{d}\kappa\mathrm{d}\xi \tag{24}$$

Let $a = 1/\kappa_l^2 + \Lambda L\xi^2/k$, $b = L\xi(1-\bar{\Theta}\xi)/k$, $\xi = z/L$, applying $\cos(\alpha) = (e^{i\alpha}+e^{-i\alpha})/2$ to Eq. (24) and there is

$$\sigma_G^2 = 1.302k^2 L \textstyle\int_0^1 C_n^2(\xi H) \displaystyle\int_0^\infty \kappa^{-\frac{11}{3}} e^{-a\kappa^2} \left[1 - \frac{1}{2}e^{ib\kappa^2} + \frac{1}{2}e^{-ib\kappa^2}\right] \cdot \left[1 + 1.802\frac{\kappa}{\kappa_l} - 0.254\left(\frac{\kappa}{\kappa_l}\right)^{7/6}\right] \mathrm{d}\xi\mathrm{d}\kappa \tag{25}$$

Since each integral of the inner integral term can be expressed as Gamma function, the scintillation index of Gaussian beam propagation on the slant path can be obtained by real part. This is shown as follows

$$\begin{aligned}\sigma_G^2 = {} & 1.302k^{\frac{7}{6}}L^{\frac{11}{6}}\int_0^1 C_n^2(\xi H)\\ & \left\{\Gamma\left(-\frac{5}{6}\right)\left[a_1^{\frac{5}{6}}-(a_1^2+b_1^2)^{\frac{5}{12}}\cos\left(\frac{5}{6}\varphi_1\right)\right]\right.\\ & +\frac{1.802}{Q_l^{1/2}}\Gamma\left(-\frac{1}{3}\right)\left[a_1^{\frac{1}{3}}-(a_1^2+b_1^2)^{\frac{1}{6}}\cos\left(\frac{1}{3}\varphi_1\right)\right]\\ & \left.-\frac{0.254}{Q_l^{7/12}}\Gamma\left(-\frac{1}{4}\right)\left[a_1^{\frac{1}{4}}-\left(a_1^2+b_1^2\right)^{\frac{1}{8}}\cos\left(\frac{1}{4}\varphi_1\right)\right]\right\}d\xi\Bigg\}\end{aligned} \tag{26}$$

where $Q_l = 10.89L/kl_0^2$, $a_1 = 1/Q_l + \Lambda\xi^2$, $b_1 = \xi(1-\bar{\Theta}\xi)$, and $\varphi_1 = \tan^{-1}(b_1/a_1)$.

This model can be converted to horizontal model while $C_n^2(\xi H)$ is a constant. Based on Eq. (22) and Eq. (23), the resulting small-scale log-irradiance fluctuation are given by

$$\sigma_{\ln y}^2(l_0,\, L) = \frac{1.272\sigma_G^2}{\left[3+2.07\left(\sigma_G^2\right)^{6/5}\right]^{\frac{5}{6}}} = \frac{0.509\sigma_G^2}{\left[1+0.69\left(\sigma_G^2\right)^{6/5}\right]^{\frac{5}{6}}} \tag{27}$$

2.3. Large-scale Scintillation Model

The large-scale log-irradiance fluctuation with inner-and outer-scale are given by

$$\begin{aligned}\sigma_{\ln x,\, l_0,\, L_0}^2 = {} & 8\pi^2k^2L\int_0^1\int_0^\infty \kappa\Phi_n(\kappa)G_x(\kappa,\, l_0,\, L_0)\\ & \exp\left[-\left(\Lambda L\kappa^2\xi^2/k\right)\right]\left\{1-\cos\left[\frac{L\kappa^2}{k}\xi\left(1-\bar{\Theta}\xi\right)\right]\right\}\mathrm{d}\kappa\mathrm{d}\xi\end{aligned} \tag{28}$$

Let $\cos(\alpha) = (e^{i\alpha} - e^{-i\alpha})/2$, and if only considering inner-scale effect, then submitting $G_x(\kappa,\, l_0)$ to Eq. (28)

$$\begin{aligned}\sigma_{\ln x,\, l_0}^2 = {} & 0.264\pi^2k^2L\int_0^1 C_n^2(\xi H)\int_0^\infty \kappa\kappa^{-\frac{11}{3}}\\ & \exp\left[-\left(\frac{1}{\kappa_l^2}+\frac{1}{\kappa_0^2}+\frac{1}{\kappa_x^2}+\frac{\Lambda L\xi^2}{k}\right)\kappa^2\right]\end{aligned}$$

$$\begin{aligned} &\cdot\left[1+1.802\frac{\kappa}{\kappa_l}-0.254\left(\frac{\kappa}{\kappa_l}\right)^{\frac{7}{6}}\right] \\ &\cdot\left[1-\frac{1}{2}e^{i\frac{b_2L}{k}\kappa^2}-\frac{1}{2}e^{-i\frac{b_2L}{k}\kappa^2}\right]\mathrm{d}\kappa\mathrm{d}\xi \end{aligned} \tag{29}$$

Let $a_2 = (k/L\kappa_l^2) + (k/L\kappa_x^2) + \Lambda\xi^2$, $b_2 = \xi(1-\bar{\Theta}\xi)$, we apply $\int_0^\infty t^{z-1}e^{-\lambda t}\mathrm{d}t = \lambda^{-z}\Gamma(z)\lambda > 0$ to Eq. (29), and educe the equation as follows, which shape is the same as Eq. (26). Hence, on the slant path, we give the closely precise expression of large-scale log-irradiance with finite inner-scale by

$$\begin{aligned} \sigma^2_{\ln x,\,l_0} =& 1.302k^{\frac{7}{6}}L^{\frac{11}{6}}\int_0^1 C_n^2(\xi H) \\ &\left\{\Gamma\left(-\frac{5}{6}\right)\left[a_2^{\frac{5}{6}}-(a_2^2+b_2^2)^{\frac{5}{12}}\cos\left(\frac{5}{6}\varphi_2\right)\right]\right. \\ &+\frac{1.802}{Q_l^{1/2}}\Gamma\left(-\frac{1}{3}\right)\left[a_2^{\frac{1}{3}}-(a_2^2+b_2^2)^{\frac{1}{6}}\cos\left(\frac{1}{3}\varphi_2\right)\right] \\ &\left.-\frac{0.254}{Q_l^{7/12}}\Gamma\left(-\frac{1}{4}\right)\left[a_2^{\frac{1}{4}}-(a_2^2+b_2^2)^{\frac{1}{8}}\cos\left(\frac{1}{4}\varphi_2\right)\right]\right\}\mathrm{d}\xi\Bigg\} \end{aligned} \tag{30}$$

where $\eta_x = L\kappa_x^2/k$, $Q_l = L\kappa_l^2/k$, $a_2 = 1/Q_l + 1/\eta_x + \Lambda\xi^2$ and $\varphi_2 = \tan^{-1}(b_2/a_2)$.

For the non-dimensional quantity η_x, as $Q_l\sigma_0^2 \gg 100$, for beam wave, based on reference [9] the longitudinal scintillation index approximately expresses as

$$\sigma_I^2(0,\,L) = 1 + \frac{2.39+5.26\bar{\Theta}}{(\sigma_0^2 Q_l^{7/6})^{1/6}} \tag{31}$$

where on slant path, the Rytov variance for beam wave defined by Eq. (14).

In the saturation regime the small-scale log-irradiance approaches $\sigma^2_{\ln y} = \ln 2$, regardless of the type of optical wave, and the longitudinal scintillation index takes the limiting form [3]

$$\sigma^2_{I,\,l}(L) = \exp(\sigma^2_{\ln I,\,l}) - 1 = \exp(\sigma^2_{\ln x} + \sigma^2_{\ln y}) - 1 \cong 1 + 2\sigma^2_{\ln x} \quad \sigma_0^2 \gg 1 \tag{32}$$

In the saturation regime for long propagating distance or strong turbulence, the geometrical optics method can be applied to large-scale irradiance fluctuations. When the geometric optics approximation is applied to Eq. (28), the large-scale log-irradiance associated with the longitudinal component under the case of finite inner scale is the form

$$\begin{aligned}\sigma^2_{\ln x,\,l_0} &= 0.652k^{\frac{7}{6}}L^{\frac{11}{6}}\int_0^1 C_n^2(\xi H)\xi^2(1-\bar{\Theta}\xi)^2\int_0^\infty \eta^{\frac{1}{6}}\exp\left[-\left(\frac{1}{Q_l}+\frac{1}{\eta_x}\right)\eta\right]\\ &\quad\cdot\left[1+1.802\left(\frac{\eta}{Q_l}\right)^{\frac{1}{2}}-0.254\left(\frac{\eta}{Q_l}\right)^{\frac{7}{12}}\right]\mathrm{d}\eta\mathrm{d}\xi\\ &\cong 0.697k^{\frac{7}{6}}L^{\frac{11}{6}}\eta_x^{\frac{7}{6}}\int_0^1 C_n^2(\xi H)\xi^2(1-\bar{\Theta}\xi)^2\mathrm{d}\xi \quad Q_l\sigma_0^2\gg 100 \end{aligned} \tag{33}$$

From weak to strong fluctuation region, based on asymptotic behavior (Eq. (31) and Eq. (33)), the parameter η_x has the form of

$$\frac{1}{\eta_x}=\frac{0.38}{1-3.21\Theta+5.29\Theta^2}+0.629Q_l^{\frac{1}{6}}\left(\frac{\sigma_{1,\,B}^{1/3}\sigma_2^2}{1+2.20\Theta^2}\right)^{\frac{6}{7}} \tag{34}$$

where $\sigma_2^2=k^{\frac{7}{6}}L^{\frac{11}{6}}\int_0^1 C_n^2(\xi H)\xi^2(1-\bar{\Theta}\xi)^2\mathrm{d}\xi$.

In the same way, when considering outer-scale, submitting $G_x(\kappa,\,L_0)$ in Eq. (7) to Eq. (28). By contrast, we can obtain the expression as follows

$$\eta_{x0}=L\kappa_{x0}^2/k=\eta_x Q_0/(\eta_x+Q_0) \tag{35}$$

where $Q_0=64\pi^2L/(kL_0^2)$, η_x is given by Eq. (34), and $\sigma^2_{\ln x,\,L_0}$ can be obtained by η_{x0} in Eq. (35) replaces η_x in Eq. (33), then the large-scale log-irradiance associated with the longitudinal component under the case of finite outer-scale is the form

$$\sigma^2_{\ln x,\,L_0}=0.697k^{\frac{7}{6}}L^{\frac{11}{6}}\eta_{x0}^{\frac{7}{6}}\int_0^1 C_n^2(\xi H)\xi^2(1-\bar{\Theta}\xi)^2\mathrm{d}\xi \tag{36}$$

2.4. The Beam Scintillation Index with Inner-scale on Slant Path

Based on the radial component of scintillation on the horizontal path, outer-scale effects in the radial component on slant path is shown as

$$\begin{aligned}\sigma^2_{I,\,r}(r,\,l_0,\,L_0) &\cong \sigma^2_{\ln I,\,r}(r,\,L)\\ &\cong 4.42\sigma^2_{1,\,B}\Lambda_e^{5/6}\left[1-1.15\left(\frac{\Lambda_e L}{kL_0^2}\right)^{1/6}\right]\frac{r^2}{W_e^2}\\ &\quad r\le W\end{aligned} \tag{37}$$

By combining all the above results, we obtain the scintillation index model with finite inner scale and outer scale effects for a Gaussian beam wave propagating on slant path, which is given by Eq. (38). In this model, however, the inner-scale effect is considered in $\sigma^2_{\ln x, l}(0, L, l_0)$ and σ^2_G, the outer-scale effect is considered in $\sigma^2_{\ln x, l}(0, L, L_0)$. On slant path, the scintillation index model with finite inner- and outer scale is shown as

$$\sigma_I^2(r, L) = \sigma^2_{\ln I, r} + \exp\left[\sigma^2_{\ln x, l_0} - \sigma^2_{\ln x, L_0} + \frac{0.509\sigma_G^2}{[1+0.69(\sigma_G^2)^{\frac{6}{5}}]^{\frac{5}{6}}}\right] - 1 \quad (38)$$

From the theory of beam propagation, when the beam radius increasing, its transfer character is approach to that of the plan wave, but when the beam radius decreasing, it transfer character is approach to that of the sphere wave. The scintillation index model with finite inner- and outer scale in Eq. (38) can be degenerated the result of plan wave propagation on the slant path when $\bar{\Theta} = 0$ and can be degenerated the result of sphere wave propagation on the slant path when $\bar{\Theta} = 1$. This indicates the result of scintillation index model is valid. Assumption atmospheric turbulence structure constant is homogeneous in transfer path Eq. (38) can be degenerated to the result

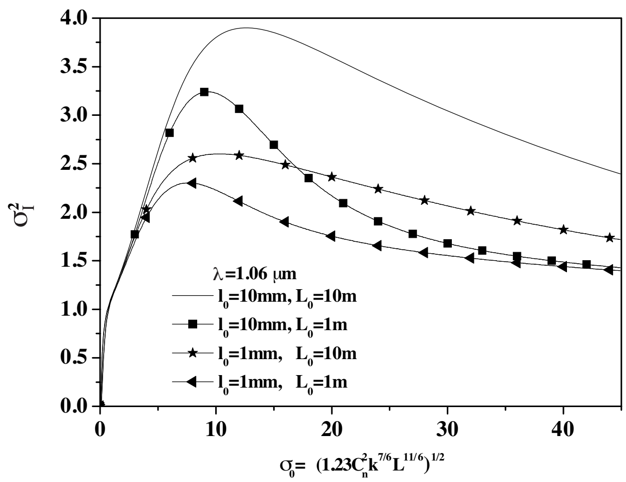

Figure 1. The scintillation index with inner-scale and outer-scale effect, $\lambda = 1.06\,\mu$m.

of horizontal path

$$\sigma_{I,bh}^2 = \exp\left[\frac{0.45\sigma_0^2 c_1^{7/6}\left[1/3-0.5\bar{\Theta}+0.2\bar{\Theta}^2\right]}{\left[1+0.914c_1\sigma_0^{12/5}\left[\frac{1/3-0.5\bar{\Theta}+0.2\bar{\Theta}^2}{0.86-0.19\bar{\Theta}+2.06\bar{\Theta}^2}\right]^{6/7}\right]^{\frac{7}{6}}} + \frac{1.272\sigma_0^2}{\left[(3+5\bar{\Theta})+2.07\sigma_0^{12/5}\right]^{5/6}}\right]-1 \tag{39}$$

where $c_1 = 3 + 5\bar{\Theta}$, it is valid under $0 \leq \sigma_0^2 < \infty$. Eq. (39) can also be obtained based on modified Rytov and Gaussian beam optical scintillation theory. This models shape is the same as Eq. (40), which is given by Hopen and Andrews. Comparing the two equations, we find the two coefficients in Eq. (40) may be misprinted.

$$\sigma_{I,bh}^2 = \exp\left[\frac{0.45\sigma_0^2 c_1^{7/6}\left[1/3-0.5\bar{\Theta}+0.2\bar{\Theta}^2\right]}{\left[1+1.51c_1\sigma_0^{12/5}\left[\frac{1/3-0.5\bar{\Theta}+0.2\bar{\Theta}^2}{0.86-0.19\bar{\Theta}+2.06\bar{\Theta}^2}\right]^{6/7}\right]^{\frac{7}{6}}} + \frac{1.272\sigma_0^2}{\left[(3+5\bar{\Theta})+1.83\sigma_0^{12/5}\right]^{5/6}}\right]-1 \tag{40}$$

3. NUMERICAL ANALYSIS AND CONCLUSIONS

On slant path, based on the turbulence atmosphere structure constant model $C_n^2(h)$ recommended by ITU-R with $C_0 = 1.7 \times 10^{-13}$, for wavelength $\lambda = 1.06\,\mu$m, $1.55\,\mu$m, $3.8\,\mu$m, $10.6\,\mu$m laser Gaussian collimated beam wave, the numerical results of scintillation index considering finite inner scale ($l_0 = 1\,$mm, $10\,$mm) and outer scale ($L_0 = 1\,$m, $10\,$m) effect with turbulence strong parameter $\sigma_0 = (1.23C_n^2 k^{7/6} L^{11/6})^{1/2}$ are given as Figures 1–4, which are calculated by Eq. (38).

These predicted results show that the inner-scale has a strong impact on beam scintillation index under moderate to strong irradiance fluctuations, and the smaller wavelength the stronger inner-scale effect, The effect of inner-scale is bigger than which of outer-scale, and under strong turbulence, the outer-scale effect is stronger, even at the case of

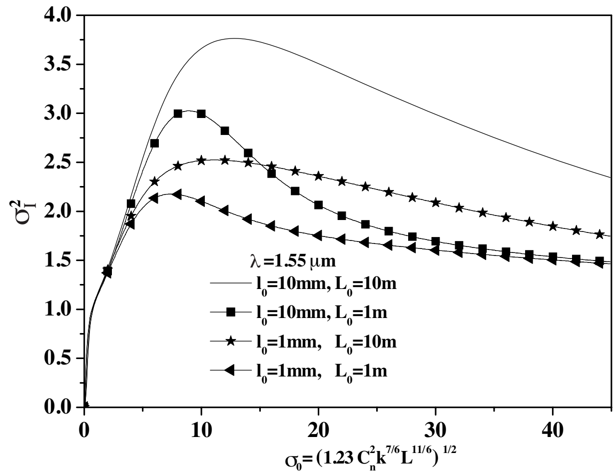

Figure 2. The scintillation index with inner-scale and outer-scale effect, $\lambda = 1.55\,\mu$m.

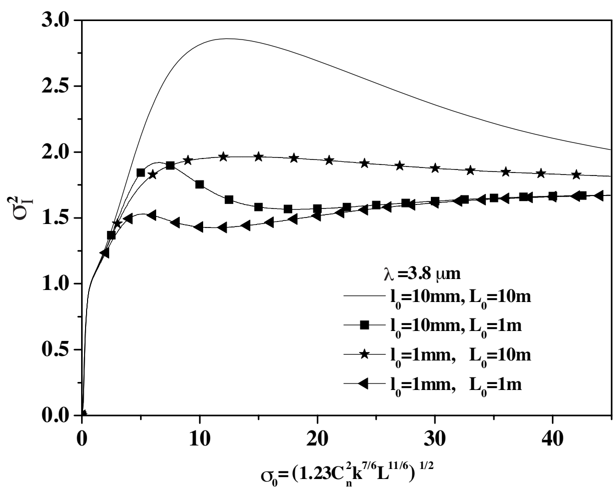

Figure 3. The scintillation index with inner-scale and outer-scale effect, $\lambda = 3.8\,\mu$m.

the large wavelength. So under strong turbulence or long propagation path, it is to consider not only the effect of inner-scale but also the outer-scale to scintillation index.

In Figure 5, open circles represent scintillation data taken form [13]. The range of inner-scales in experimental data is over the

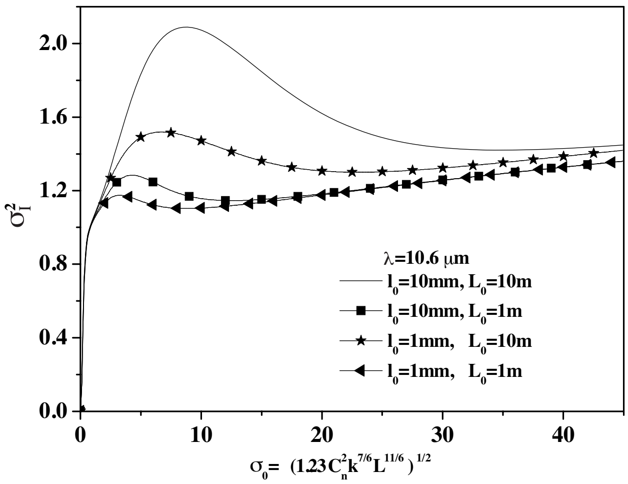

Figure 4. The scintillation index with inner-scale and outer-scale effect, $\lambda = 10.6\,\mu$m.

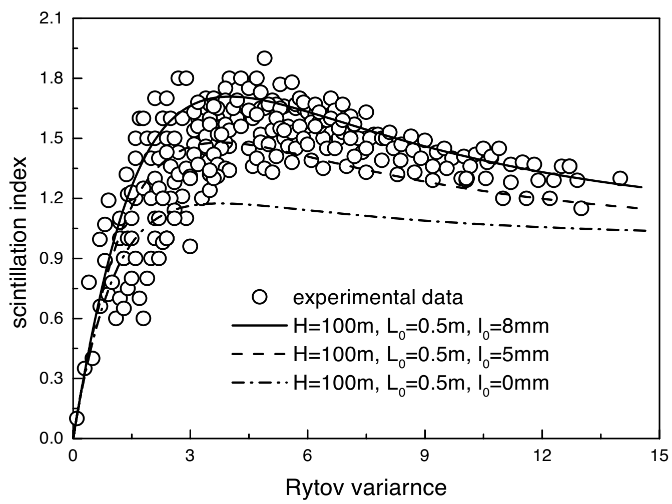

Figure 5. Comparisons the results of considering the effects of inner- and outer-scale with the experimental data.

intervals $3\,\text{mm} < l_0 < 7\,\text{mm}$. For validating the results in this paper, Figure 5 shows the comparisons of the results by considering the effects of inner- and outer-scale with the experimental data. It is shown that the numerical results of the scintillation with zone inner-scale is smaller than the experimental data, and the results of considering inner-and outer-scales is drive to experimental data. This is consistent with theories analysis [11]. Figure 5 illustrates considering the inner- and outer-scales, theoretical results of laser beam propagation on slant path from weak fluctuation area to the saturated area to track the experimental data quite closely.

4. CONCLUSIONS

This model of the scintillation index with finite inner- and outer-scale for laser beam wave propagating through atmospheric turbulence medium on slant path is developed under the assumption that small-scale irradiance fluctuations are modulated by large-scale irradiance fluctuations and it is valid under moderate to strong irradiance fluctuations on slant path. On slant path, the scintillation indexes with finite inner-scale are general smaller than the results on horizontal path. This scintillation index model for laser beam propagation in atmosphere turbulence is significant for the visible and infrared imaging, laser tracking, controlling and guiding, and laser satellite-Earth communication.

ACKNOWLEDGMENT

Supported by National Natural Science Foundation of China (60771038/F0104).

REFERENCES

1. Tatarskii, V. I., *Wave Propagation in a Turbulent Medium*, McGraw-Hill, New York, 1961.
2. Chernov, L. A., *Wave Propagation in a Random Medium*, McGraw-Hill, New York, 1960.
3. Ishimaru, A., *Wave Propagation and Scattering in Random Media*, Academic Press, New York, 1978.
4. Jakeman, E., "Enhanced backscattering through a deep random phase screen," *J. Opt. Soc. Am. A*, Vol. 5, 1638–1648, 1988.
5. Hill, R. J., "Theory of saturation of optical scintillation by strong turbulence, plane-wave variance and covariance and spherical-wave covariance," *J. Opt. Soc. Am. A*, Vol. 72, 212–222, 1981.
6. Hill, R. J. and S. F. Clifford, "Theory of saturation of optical scintillation by strong turbulence for arbitrary refractive-index spectra," *J. Soc. Am. A*, Vol. 71, 675–686, 1981.
7. Andrews, L. C., et al., "Theory of optical scintillation," *J. Opt. Soc. Am. A*, Vol. 16, 1417–1429, 1999.

8. Guo, L.-X., Z.-M. Luo, and Z.-S. Wu, "A study of optical scintillation in the atmospheric turbulence by using modification of the Rytov method," *Chin of Electronic*, Vol. 10, 300–304, 2001.
9. Wu, Z.-S., et al., "Study on scintillation of optical wave propagation in the slant path through the atmospheric turbulence," *Chinese Journal of Radio Science*, Vol. 17, 254–268, 2002.
10. Fante, R. L., "Electromagnetic beam propagation in turbulent media," *Proceedings of the IEEE*, Vol. 63, 1669–1688, 1975.
11. Fante, R. L., "Inner-scale size effect on the scintillations of light in the turbulent atmosphere," *J. Opt. Soc. Am. A*, Vol. 73, 277–281, 1983.
12. Andrews, L. C., R. L. Phillips, C. Y. Hopen, et al., "Theory of optical scintillation: Gaussian-beam wave model," *Waves Random Media*, Vol. 11, 271–291, 2001.
13. Consortini, A., F. Cochetti, et al., "Inner scale effect on irradiance variance measured for weak-to-strong atmospheric scintillation," *J. Opt. Soc. Am. A*, Vol. 10, 2354–2362, 1993.
14. Miller, W. B., J. C. Ricklin, and L. C. Andrews, "Effect of the refractive index spectral model on the irradiance variance of a Gaussian beam," *J. Opt. Soc. Am. A*, Vol. 11, 2719–2726, 1994.
15. Hopen, C. Y. and L. C. Andrews, "Optical scintillation of a Gaussian beam in moderate-to-strong irradiance fluctuations," *SPIE*, Vol. 4, 142–150, 1999.
16. Ren, K., X. B. Ren, X. D. Zhang, et al., "Experimental investigation of relationship between the object and image distance," *PIERS Online*, Vol. 3, No. 3, 286–288, 2007.
17. Jiao, C.-Q. and J.-R. Luo, "Beam-wave Coupling in a double-beam gyrotron traveling wave amplifier," *PIERS Proceeding*, 2203–2206, March 2007.
18. Song, K. S., Y. Z. Zhang, et al., "Inverse data modeling for the optical properties of the entropic lake from reflectance spectra in Nanhu Lake of Changchun, China," *J. of Electromagn. Waves and Appl.*, Vol. 21, No. 7, 889–898, 2007.
19. Jandieri, G. V., A. Ishimaru, et al., "Model computations of angular power spectra for anisotropic absorptive turbulent magnetized plasma," *Progress In Electromagnetics Research*, PIER 70, 307–328, 2007.
20. Bhunek, I. and P. Fiala, "Turbulence modeling of air flow in the heat accumulator layer," *PIERS Online*, Vol. 2, No. 6, 662–666, 2006.

21. Palmer, R. D. and L. Cheong, "Review of atmospheric boundary layer observations using the turbulent eddy profiler," *PIERS Proceeding*, Tokyo, August 2006.
22. Kuramoto, A., A. Hori, and C. Fujieda, "Laser speckle imaging of a finger by scattered light optic," *PIERS Online*, Vol. 3, No. 6, 832–835, 2007.
23. Yan, Y. and J. G. Xin, "Beam propagation in laser scattering communication," *PIERS Proceeding*, 1191–1193, March 2007.
24. Talhi, R., A. Leberere, F. Li, and F. Csten, "Prediction of some ionospheric effects on radio-waves propagation," *PIERS Proceeding*, 76, August 2007.
25. Li, F., F. Lefeuvre, M. Parrot, and R. Talhi, "Low latitude inonspheric turbulence observed by the micro-satellite DEMETER," *PIERS Proceeding*, 79, August 2007.
26. Sarkat, S. K., "Wave propagation phenomena in troposphere over the Indian subcontinent," *PIERS Proceeding*, Tokyo, August 2006.
27. Cossmann, S. M. and E. J. Rothwell, "Transient reflection of plane waves from a lorentz medium half space," *J. of Electromagn. Waves and Appl.*, Vol. 21, No. 10, 1289–1302, 2007.
28. Nyobe, E. N. and E. Pemha, "Propagation of a laser beam through a plane and free turbulent heated air flow: Determination of the stochastic characteristics of the laser beam random direction and some experimental results," *PIERS Online*, Vol. 3, No. 6, 832–835, 2007.
29. Zhou, D. K., "Monitouring the earth, ocean, and atmosphere with hyperspectral remote sensors," *PIERS Online*, Vol. 2, No. 6, 694–697, 2006.
30. Georgiadou, E. M., A. D. Panagopoulos, and J. D. Kanellopoulos, "Millimeter wave pulse propagation through distorted raindrops for fixed wireless access channels," *J. of Electromagn. Waves and Appl.*, Vol. 20, 1235–1248, 2006.
31. "On propagation data and prediction methods required for the design of space-to-earth and earth-to-space optical communication systems," ITU-R. Document 3J/31-E, Radio Communication Study Group Meeting, Budapest, July 2001.
32. Andrews, L. C., et al., "Scintillation model for a satellite communication link at large zenith angles," *Optical Engineering*, Vol. 39, 3272–3280, 2000.